



# Fast predictions of aerodynamic coefficients and heat flux in Hypersonic vehicles

Vinícius Hagemeyer Chiumento<sup>1</sup>, Pedro Paulo Batista de Araújo<sup>2</sup>, Fábio Henrique Eugênio Ribeiro<sup>3</sup>, Angelo Passaro, Lucas Galembeck, Johan Steelant

### **Abstract**

HipeX is a fast and lightweight aerothermodynamic analysis tool developed to estimate aerodynamic coefficients and surface heat fluxes on hypersonic vehicles using local surface inclination methods. The solver combines classical techniques such as the tangent-wedge method, the modified Newtonian approach, and Prandtl-Meyer expansions to evaluate pressure distributions across arbitrary geometries. Heat flux predictions are derived using similarity-based boundary-layer models, with compressibility effects accounted for through Eckert's reference temperature formulation. A key feature of HipeX is its blended boundary-layer model, which transitions from laminar to turbulent flow based on local Reynolds number. Validation against benchmark CFD data for the HEXAFLY-INT experimental configuration shows that HipeX provides reliable aerodynamic and thermal load estimates.

**Keywords:** Aerothermodynamics, Heat transfer, Aerodynamics

#### **Nomenclature**

Latin A – Panel area

 $C_f$  – Skin friction coefficient

 $C_p$  – Specific heat at constant pressure

 $\vec{C_P}$  – Pressure coefficient  $\dot{M}$  – Mach number

P - Pressure

Pr - Prandtl Number

 $q_w$  – Convective heat flux  $Q_{tot}$  – Total heat rate

Re - Reynolds Number

S - Reference area

St – Stanton number T – Temperature

Tu - Turbulent intensity

u – Velocity

 $x_l\,$  – Local distance from the leading edge

 $\beta$  – Oblique shock wave angle

 $\gamma$  – Specific heat ratio ( $C_p/C_v$ )

 $\gamma_{it}$  – Intermittency factor  $\mu$  – Dynamic viscosity

 $\nu(M)$  – Prandtl–Meyer function

 $\rho$  – Density

 $\sigma$  – Stefan–Boltzmann constant

 $\varepsilon$  – Surface emissivity

Subscripts

e - Properties at the edge of the boundary layer

 $w\,$  – Wall properties

 $\infty$  – Free-stream properties

HiSST-2025-0171 Copyright © 2025 by the author(s)

<sup>&</sup>lt;sup>1</sup>Institute for Advanced Studies, Trevo Coronel Aviador José Alberto Albano do Amarante, 1 – São José dos Campos – SP – Brazil, vini.hagemeyer@gmail.com

<sup>&</sup>lt;sup>2</sup>Institute for Advanced Studies, Trevo Coronel Aviador José Alberto Albano do Amarante, 1 – São José dos Campos – SP – Brazil, araujo.projects@gmail.com

<sup>&</sup>lt;sup>3</sup>Institute for Advanced Studies, Trevo Coronel Aviador José Alberto Albano do Amarante, 1 – São José dos Campos – SP – Brazil, henriquefher@fab.mil.br

<sup>&</sup>lt;sup>4</sup>Institute for Advanced Studies, Trevo Coronel Aviador José Alberto Albano do Amarante, 1 – São José dos Campos – SP – Brazil, angelopassaro@gmail.com

<sup>&</sup>lt;sup>5</sup>Institute for Advanced Studies, Trevo Coronel Aviador José Alberto Albano do Amarante, 1 − São José dos Campos – SP – Brazil, galembecklg@fab.mil.br

<sup>&</sup>lt;sup>6</sup>European Space Agency (ESTEC), Keplerlaan 1, 2201AZ Noordwijk, The Netherlands, Johan.Steelant@esa.int

### 1. Introduction

Local surface inclination methods are of significant importance in the design of hypersonic vehicles, as they provide rapid and reasonably accurate estimations of aerodynamic forces and heat transfer. These methods enable swift design iterations and optimizations during the early stages of development, when detailed computational fluid dynamics (CFD) simulations can be prohibitively time-consuming. This paper presents recent improvements to a computational tool named HipeX for aerodynamics and heat transfer analysis using local surface inclination methods [1] [2].

Viscous contributions are estimated using similarity solutions for boundary layers, employing correlations derived for flat plates aligned with local streamlines. The boundary layer may be either laminar or turbulent. While assuming a fully turbulent boundary layer provides a conservative estimate, it often leads to overprediction of skin friction drag and surface heat flux. This conservatism results in oversized thermal protection systems, which in turn increases propulsion requirements and ultimately impacts the overall vehicle mass and fuel consumption [3].

To enhance the fidelity of the physical model, transitional boundary layer modeling is employed. In this approach, a critical Reynolds number is calculated to determine the onset of transition from laminar to turbulent flow. The surface is then modeled using a composite approach, combining laminar and turbulent boundary layer characteristics over a defined transition region [4]. This methodology directly influences system-level metrics such as structural mass, insulation thickness and fuel margin. Incorporating transition effects is therefore essential for optimizing vehicle performance and achieving a balanced trade-off between design conservatism and mission efficiency.

## 1.1. Methodology

The aerodynamic coefficients are determined using a hybrid engineering-level approach. This method selectively applies the most suitable model among the implemented ones (tangent-wedge, modified Newtonian, or Prandtl-Meyer expansion) based on the local surface inclination relative to the freestream velocity vector. The framework supports two computational modes for handling complex geometries: the first considers each panel independently, while the second accounts for aerodynamics by using flow properties from upstream panels to inform calculations for downstream panels.

Wall shear stress and surface friction are modeled using Eckert's reference enthalpy method, applicable to both laminar and turbulent boundary layers. A pre-calculated critical Reynolds number governs the transition from laminar to turbulent flow. The local Reynolds number is evaluated based on the distance from the panel to the estimated leading edge along a streamline. This leading-edge location is approximated by analyzing the spatial relationship between the centroid of the panel in question and the centroids of adjacent upstream panels. The surface heat flux is then derived from the computed skin friction coefficient.

The solver, HipeX, processes unstructured surface meshes provided in the Standard Triangulation Language (STL) format. Topological information, such as panel adjacency, is precomputed and cached to significantly accelerate coefficient calculations over varying angles of attack. The resulting surface distributions of aerodynamic pressure and convective heat flux are exported in the Visualization Toolkit (VTK) file format for post-processing. Atmospheric properties (pressure, density, temperature) are determined as a function of altitude using the 1976 U.S. Standard Atmosphere model [5].

#### 1.1.1. 3D Shock Expansion Method

The shock-expansion method employed here is based on local surface inclination techniques, notably the tangent-wedge approach. These methods rely solely on the local inclination angle to determine whether the flow is undergoing compression or expansion, from which the pressure coefficient is subsequently derived. In the tangent-wedge method, aerodynamic properties over a given panel are computed by assuming an oblique shock forms from the interaction between the panel and the incident free-stream. In this mode, each panel is treated independently. In contrast, the full shock-expansion method incorporates the flow conditions resulting from upstream panels when determining the pressure and thermal loads on downstream panels. A known limitation of both methods is that they neglect reflected shock waves, which limits their applicability in regions with complex shock interactions.

The pressure coefficient used throughout this analysis is defined as:

$$C_p = \frac{P_w - P_\infty}{0.5 \ \rho_\infty \ u_\infty^2},\tag{1}$$

where  $P_w$  is the wall (local surface) pressure, P, rho, u are the free-stream pressure, density and velocity, respectively. According to the inclination of the panel, the appropriate methodology is selected to compute the flow properties. If the shock wave is not attached to the panel, the modified Newtonian method is used [6], which computes the pressure coefficient using:

$$C_p = C_{p,max} \sin^2 \theta, \tag{2}$$

where  $\theta$  is the local inclination angle of the panel relative to the free-stream direction. The maximum pressure coefficient  $Cp_{max}$  is given by:

$$C_{p,max} = \frac{2}{\gamma M_1^2} \left( \left[ \frac{(\gamma + 1)^2 M_1^2}{4\gamma M_1^2 - 2(\gamma - 1)} \right]^{\frac{\gamma}{\gamma - 1}} \left[ \frac{1 - \gamma + 2\gamma M_1^2}{\gamma + 1} \right] - 1 \right), \tag{3}$$

where  $M_1$  is the upstream Mach number, and  $\gamma$  is the specific heat ratio. This method yields better results for blunt vehicles. In this study, the modified Newtonian method is employed in regions with high local inclination angles where detached shocks are expected. For attached shocks, the pressure and downstream Mach number after the shockwave  $(M_2)$  are obtained by solving the  $\beta-\theta-M$  relation:

$$\tan\theta = 2\cot\beta \left[\frac{M_1^2 sin^2\beta - 1}{M_1^2(\gamma + cos2\beta) + 2}\right], \tag{4}$$

where  $\beta$  is the shock wave angle. The Mach number downstream of the shock is given by:

$$M_2 = \frac{1}{\sin(\beta - \theta)} \sqrt{\frac{1 + 0.5(\gamma - 1)(M_1 \sin \beta)^2}{\gamma (M_1 \sin \beta)^2 - 0.5(\gamma - 1)}}.$$
 (5)

The maximum flow deflection angle max for which the shock remains attached can be estimated

$$eta_{max} = \arccos\left[rac{\sqrt{(A_1 = \sqrt{A_2 A_3} - M_1^2 + 4)/\gamma}}{2M_1}
ight],$$
 (6)

where  $A_1=3M^2$  ,  $A_2=\gamma+1$  e  $A_3=8\gamma M^2+\gamma M^4-8M^2+M^4+16$ . The Prandtl–Meyer expansion is applied to surfaces with negative deflection angles, corresponding to flow expansion rather than compression [7]. The flow properties downstream of the expansion are calculated using the Prandtl-Meyer function  $\nu(M)$  , given by:

$$\nu(M) = \sqrt{\frac{\gamma+1}{\gamma-1}} \cdot \tan^{-1}\left(\sqrt{\frac{\gamma-1}{\gamma+1}(M^2-1)}\right) - \tan^{-1}\left(\sqrt{M^2-1}\right). \tag{7}$$

To determine the Mach number after expansion, an iterative method is used to solve  $\theta = \nu(M_2) - \nu(M_1)$ . The Prandtl-Meyer function has a maximum value, corresponding to the maximum deflection angle before the expansion wave becomes invalid. The maximum turning angle ( $\nu_{max}$ ) is given by:

$$\nu_{\mathsf{max}} = \frac{\pi}{2} \left( \sqrt{\frac{\gamma + 1}{\gamma - 1}} - 1 \right) - \nu(M_1). \tag{8}$$

The Prandtl–Meyer method provides a good representation of the physical phenomena, but it can produce a nonphysical solution if the panel has high inclination angles. To address this limitation and maintain physical consistency and numerical stability, HipeX restricts the local expansion angle to 50% of the theoretical maximum deflection angle. This approach ensures reliable pressure and velocity predictions, avoiding spurious results associated with excessive expansion inputs. When it is not possible to solve the Prandtl–Meyer equation, the pressure coefficient is estimated using the Gaubeaud formula [8], given by:

$$Cp = \frac{2}{\gamma M_{\infty}^2} \left[ \left( \frac{2}{\gamma + 1} \right)^{1.4} \left( \frac{1}{M_{\infty}} \right)^{2.8} \left( \frac{2\gamma M_{\infty}^2 - (\gamma - 1)}{\gamma + 1} \right) - 1 \right].$$
 (9)

For each panel an appropriate method is selected. All the implemented methods to estimate the pressure coefficient and the associated flow properties over a panel are summarized in Table 1.

Panel Condition	Method	Governing Equation(s)	Notes
Detached shock (blunt body)	Modified Newtonian	Eq. 2	Used for large deflections. Assumes detached shock.
Attached shock (compression)	Oblique Shock Relations	Eq. 4 and 5	Accurate for sharp leading edges and moderate deflections.
Expansion region	Prandtl–Meyer Expansion	Eq. 7	For panels with flow turning away (expansion).
Expansion (empirical)	Gaubeaud Empirical Model	Eq. 9	Used when Prandtl-Meyer solution fails.
Neutral or small inclination	Free-stream assumption	Cp = 0	No compression or expansion effects assumed.

Table 1. Summary of Methods for Estimating and Flow Properties

#### 1.2. Viscous model

The HipeX framework models the boundary layer using a compressible similarity solution that accounts for both laminar and turbulent regimes. To incorporate compressibility effects, the Eckert reference temperature model [9] is employed. The reference temperature  $T^*$  is given by:

$$T^* = T_e \left( 0.5 + 0.5 \frac{T_w}{T_e} + 0.044 r M^2 \right), \tag{10}$$

where  $T_e$  is the temperature at the edge of the boundary layer,  $T_w$  is the wall temperature, and r is a flow regime-dependent coefficient,  $r=Pr^{1/3}$  for turbulent flow and and  $r=Pr^{1/2}$  for laminar flow. The local Reynolds number is computed by:

$$Re_x = \frac{\rho_e u_e x_l}{\mu_e},\tag{11}$$

where  $x_l$  is the local distance from the leading edge in the streamline direction, u is the velocity and  $\mu$  is the viscosity. The skin friction coefficient,  $C_f$ , is then calculated depending on the flow regime:

Laminar flow:

$$C_f = \frac{0.664}{\sqrt{Re_x}}. (12)$$

Turbulent flow:

$$C_f = \frac{T_e}{T^*} \frac{0.451}{\left(\log_{10}(0.056Re_x(T/T^*)^{1.67})\right)^2}.$$
 (13)

The heat flux  $q_w$  is estimated by:

$$q_w = St\rho_e u_e C_p (T_{aw} - T_w), \tag{14}$$

where  $C_p$  is the specific heat at constant pressure, and  $T_{aw}$  is the adiabatic wall temperature and St is the Stanton number:

$$St = \frac{C_f}{2Pr^{2/3}}. ag{15}$$

The adiabatic wall temperature is given by:

$$T_{aw} = T_e(1 + 0.2rM^2). (16)$$

Transition between laminar and turbulent boundary layers is modeled using a critical Reynolds number,  $Re_{cr}$ , determined empirically by [10]:

$$\log_{10}(Re_{cr}) = 6.421 \cdot \exp\left(1.209 \times 10^{-4} \cdot M^{2.642}\right). \tag{17}$$

This transition model allows HipeX to estimate where the flow shifts from laminar to turbulent as a function of Mach number and streamline distance. After this point, the laminar and turbulent boundary layers are blended using the intermittency factor, which ranges from 0 (fully laminar) to 1 (fully turbulent) [3] [4]. The effective skin friction coefficient is calculated using:

$$C_f = \gamma_{it} C_{f_{\text{turbulent}}} + (1 - \gamma_{it}) C_{f_{\text{laminar}}}.$$
 (18)

The intermittency factor  $\gamma_{it}$  is modeled by:

$$\gamma_{it} = 1 - exp(-\hat{n}\sigma(Re_x - Re_{cr})^2), \tag{19}$$

where the spot production parameter ( $\hat{n}\sigma$ ) is given by:

$$\hat{n}\sigma = 1.5 \cdot 10^{-11} T u_{\infty}^{7/4} (1 + 0.58M^{0.2})^{-2}, \tag{20}$$

where  $Tu_{\infty}$  is the turbulent intensity, assumed to be 0.5%. In addition to convective heat transfer, radiative heat transfer becomes significant in hypersonic flows, especially at high altitudes and for vehicles experiencing strong shock layers. Radiation originates from the high-temperature gas in the shock layer and can contribute notably to the surface heat flux. The net radiative heat flux to the surface is given by:

$$q_{\mathsf{rad}} = \varepsilon \sigma \left( T_{amb}^4 - T_w^4 \right). \tag{21}$$

The total surface heat flux becomes the sum of convective and radiative contributions:

$$Qw_{tot} = Qw_{conv} + Qw_{rad}. (22)$$

Under specific conditions, radiative and convective heat fluxes can balance each other such  $Qw_{tot}=0$ . This implies that the surface is in thermal equilibrium and experiences no net heat gain or loss. Such a condition may occur in carefully designed thermal protection systems or in high-altitude hypersonic flight where radiative cooling is strong enough to offset convective heating. However, this balance is generally rare and typically requires high surface emissivity and extreme flow conditions.

To evaluate the total thermal load experienced by the vehicle, the local surface heat fluxes are integrated over the wet area of the body. The total heat rate  $Q_{tot}$  is calculated by:

$$Q_{tot} = \sum_{i=0}^{n_{panel}} Qw_i A_i, \tag{23}$$

where  $A_i$  is the area of panel i.

The main steps of the HipeX computational pipeline are summarized as follows:

- 1. Read the mesh and compute connectivity information;
- 2. For each condition in the trajectory list:
  - (a) Compute the atmospheric conditions at the current flight altitude;
  - (b) Rotate the mesh to the current angle of attack;
- 3. Compute the inviscid surface properties using the shock-expansion method;
- 4. Compute viscous effects, including boundary layer and surface heat fluxes;
- 5. Integrate the surface pressure and shear stress to obtain aerodynamic coefficients;
- 6. Store results and proceed to the next trajectory condition.

#### 2. Aerodynamic predictions

To validate the HipeX framework and assess its predictive accuracy, we employ the HEXAFLY-INT configuration as a benchmark case. HEXAFLY-INT (High-Speed Experimental Flight – International) is an international consortium designed to investigate sustained hypersonic cruise at Mach 7–8 [11]. The vehicle features a blended lifting-body design optimized for high aerodynamic efficiency and thermal protection during high-enthalpy atmospheric flight. The configuration has been extensively studied in wind tunnel experiments and computational simulations, providing a reliable reference for validating aerothermodynamic models.

The physical dimensions and aerodynamic reference values used in this study are as follows: the reference area (S) is  $2.52 \, \text{m}^2$ , the wingspan is  $1.24 \, \text{m}$ , the overall length is  $3.29 \, \text{m}$ , and the moment reference length is  $(1,455;0;0,12) \, \text{m}$  [12]. Figure 1 shows a schematic of the HEXAFLY-INT configuration used in this benchmark, including its main geometric characteristics and control surfaces.

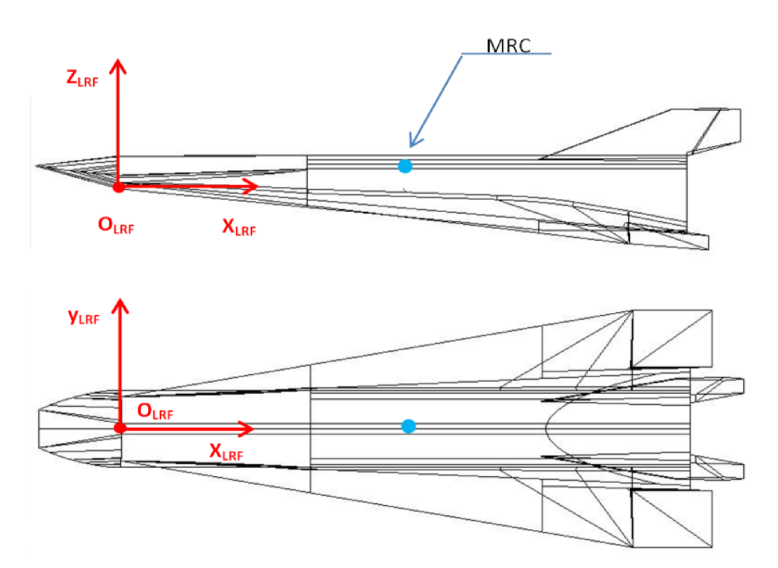


**Fig 1.** Drawing of HEXAFLY-INT, adapted from [13].

Figures 2 and 3 show the aerodynamics coefficients predicted by Hipex compared to CFD results from [14] for M = 7 and M = 6, respectively. HipeX over-predicts the drag at high angles of attack. Under this condition, the boundary layer transition occurs near the rear of the vehicle, resulting in only a small increase in drag for the blended solution compared to the fully laminar solution. For the Mach 6 case (Figure 3), the discrepancies in drag and lift are more proportional, leading to a better prediction of the aerodynamic efficiency (L/D). In all cases, the predicted position of the center of pressure  $(X_{cp})$  remains within 10% of the CFD data. These results are consistent with previous findings using the tangent-wedge method [1].

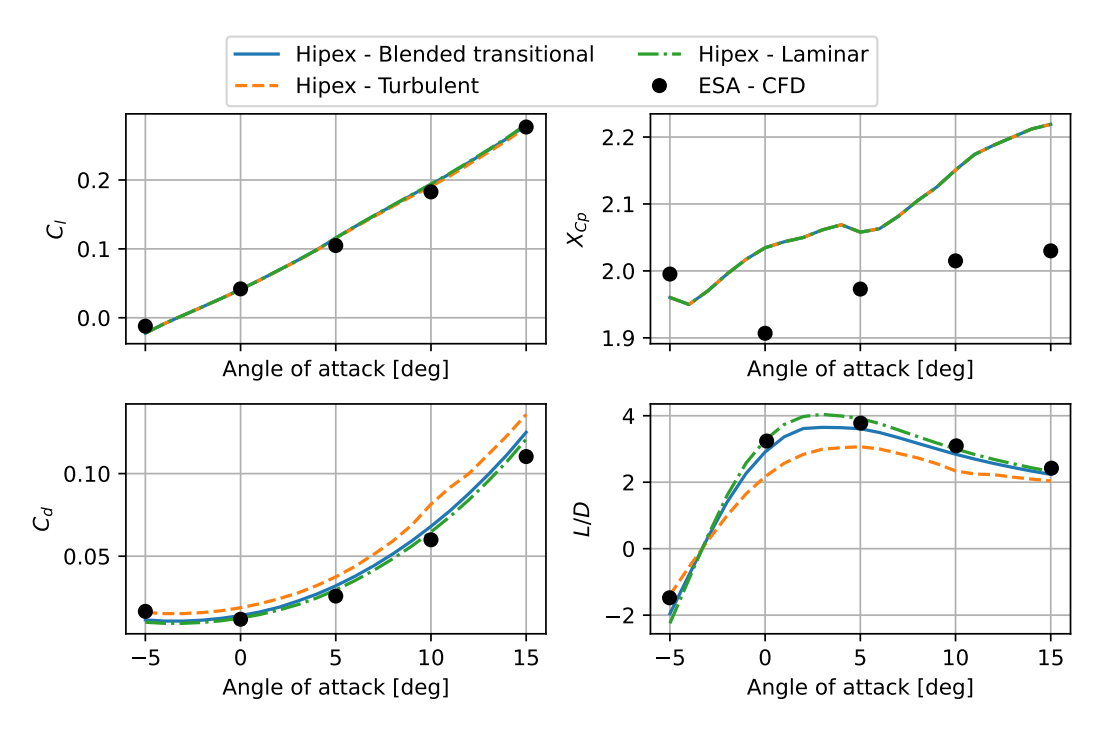


**Fig 2.** Comparison of HipeX prediction of aerodynamics coefficients and [14] for M = 7 and 27.9 km of altitude.

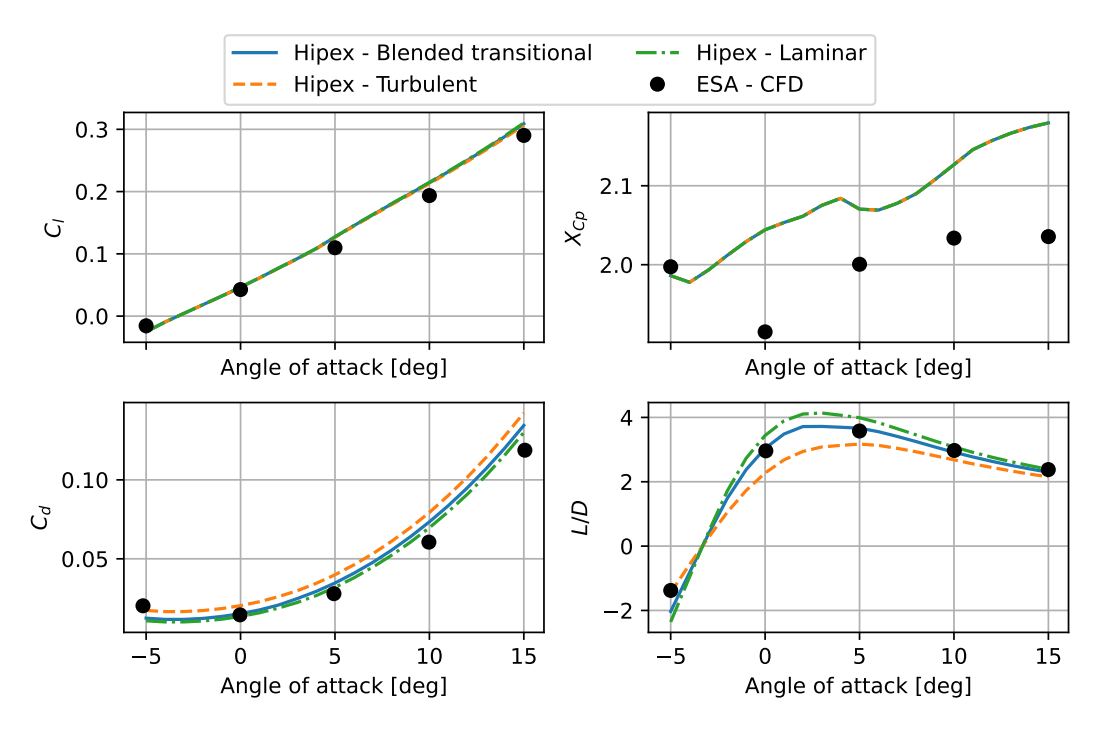


**Fig 3.** Comparison of HipeX prediction of aerodynamics coefficients and [14] for M = 6 and 27.6 km of altitude.

The trajectory analyzed, described in Table 2, extends down to Mach 4.8. For lower Mach numbers, the methods implemented in HipeX are known to provide less accurate results. Along the analyzed trajectory points, the aerodynamic efficiency predicted by HipeX agrees very well with the CFD data from [15] and [16], as shown in figure 4. At higher altitudes, the flow is predominantly laminar, causing the blended solution to yield results very close to the fully laminar case. As expected, the blended solution generally provides better results than either the pure laminar or fully turbulent assumptions.

**Table 2.** Trajectory with critical points [16].

	Tempo [s]	Altitude [m]	Mach	AoA (deg)	sigma(flap)
EFTV-065	273.5	49942	07.07	6.83	-5.46
EFTV-066	288.14	37716.85	7.46	12	-15.44
EFTV-067	290.39	35947.24	7.5	12	-15.39
EFTV-068	294.44	33059.99	7.5	12	-15.38
EFTV-069	300.52	29936.43	7.25	12	-15.72
EFTV-070	305.49	28652.17	7.1	3.62	-2.02
EFTV-071	309.55	28040.09	07.03	1.63	-0.68
EFTV-072	318.37	27461.55	6.88	-0.66	0.41
EFTV-073	350	27444.96	6.42	-1.63	0.64
EFTV-074	500.05	28854.96	4.8	0.51	-2.25

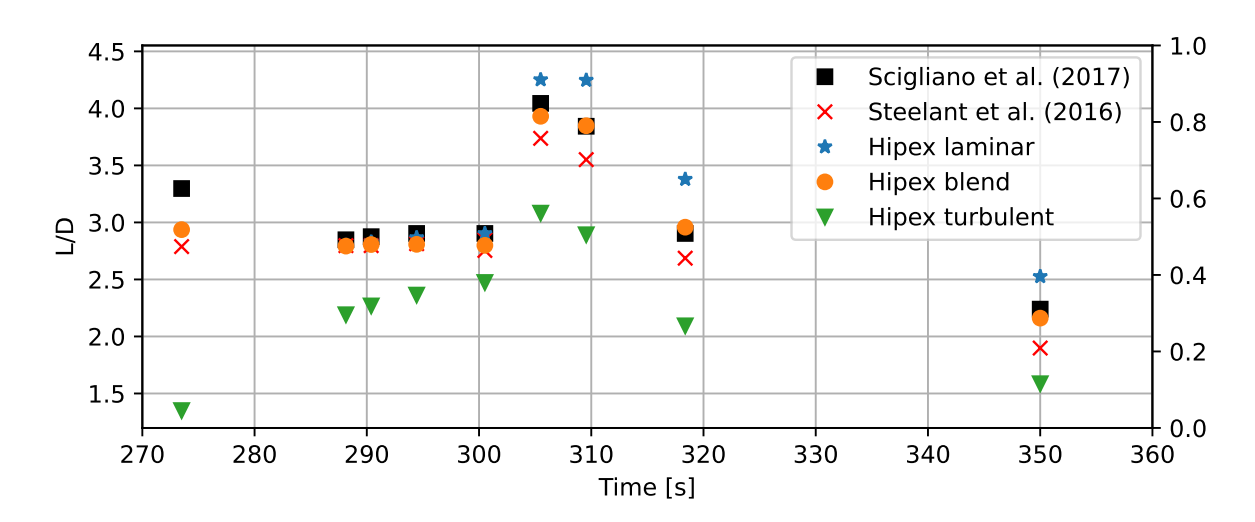
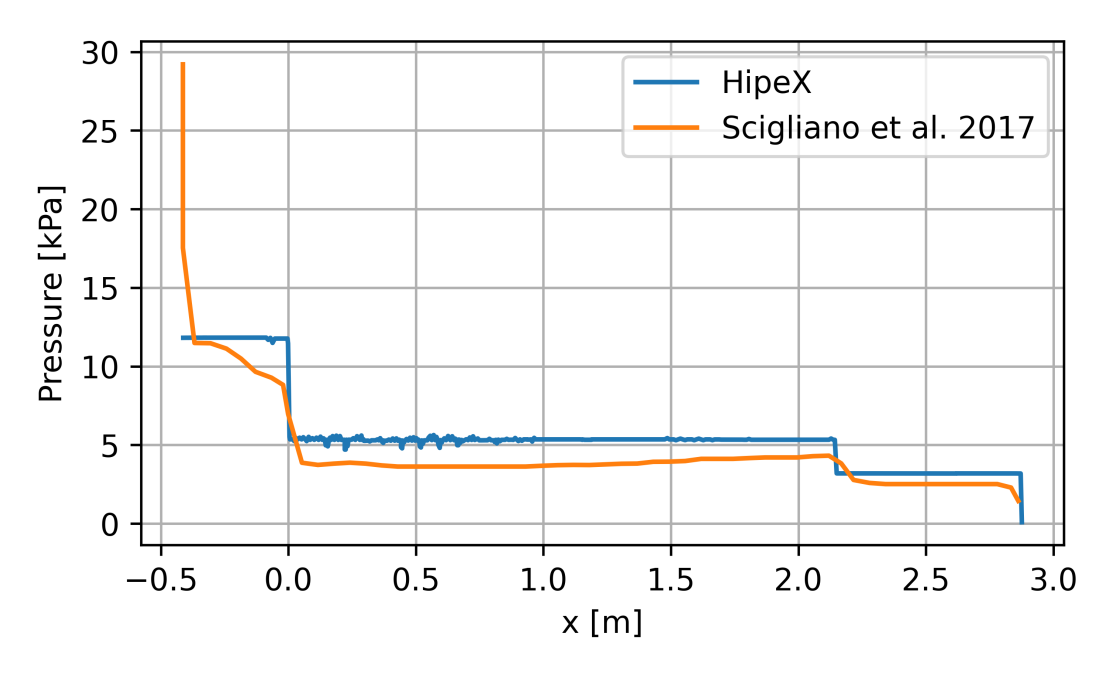


Fig 4. L/D along the flight trajectory by [16].

Figure 5 shows a comparison of the pressure distribution along the vehicle centerline. Except for the leading edge, the pressure profile predicted by HipeX shows similar behavior to the CFD results. The discrepancy at the nose is likely because the STL model used in this HipeX analysis has a perfectly sharp leading edge, whereas the original HEXAFLY-INT geometry has a 2 mm rounded edge. A similar effect is observed on the wing, where the abrupt change in the pressure distribution is caused by the aileron deflection.



**Fig 5.** Pressure distribution for M = 7.5, AoA = 12 degrees and 35.9 km of altitude.

# 3. Aerodynamic Heating

The surface temperature adopted in the following results corresponds to the equilibrium temperature, defined by the condition where the convective heat flux equals the radiative heat flux. The radiative heat flux is computed assuming an emissivity equal to 0.4. Figure 6 illustrates the surface temperature distribution for Case EFTV-069 in Table 2 and compares the HipeX solution with [17]. For the laminar case at Mach 7.5, altitude 35.9 km and angle of attack of 12 degrees, HipeX predicts a heat flux that closely matches the CFD reference. The comparison is presented in Figure 7, and corresponds to Case EFTV-067 in Table 2.

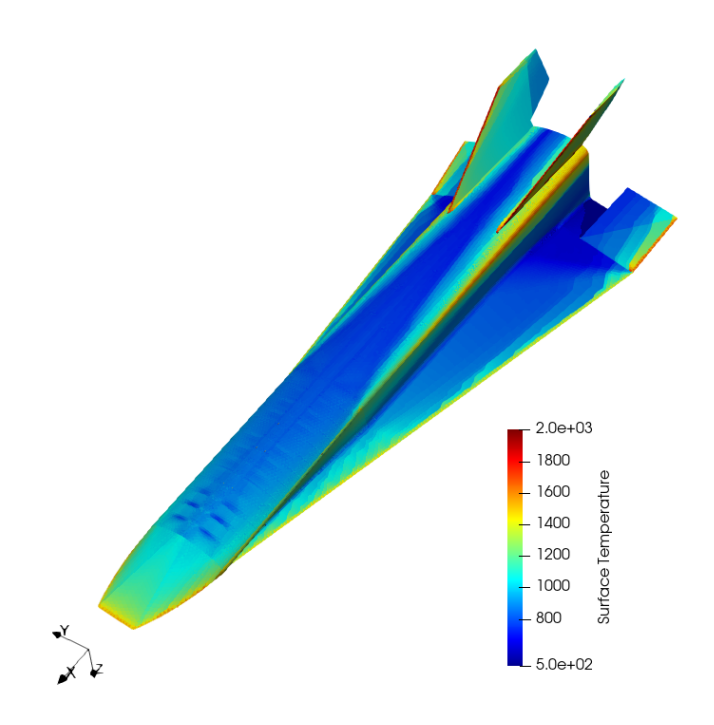


**Fig 6.** Radiative equilibrium temperature for M = 7.25 and 29.9 km of altitude.

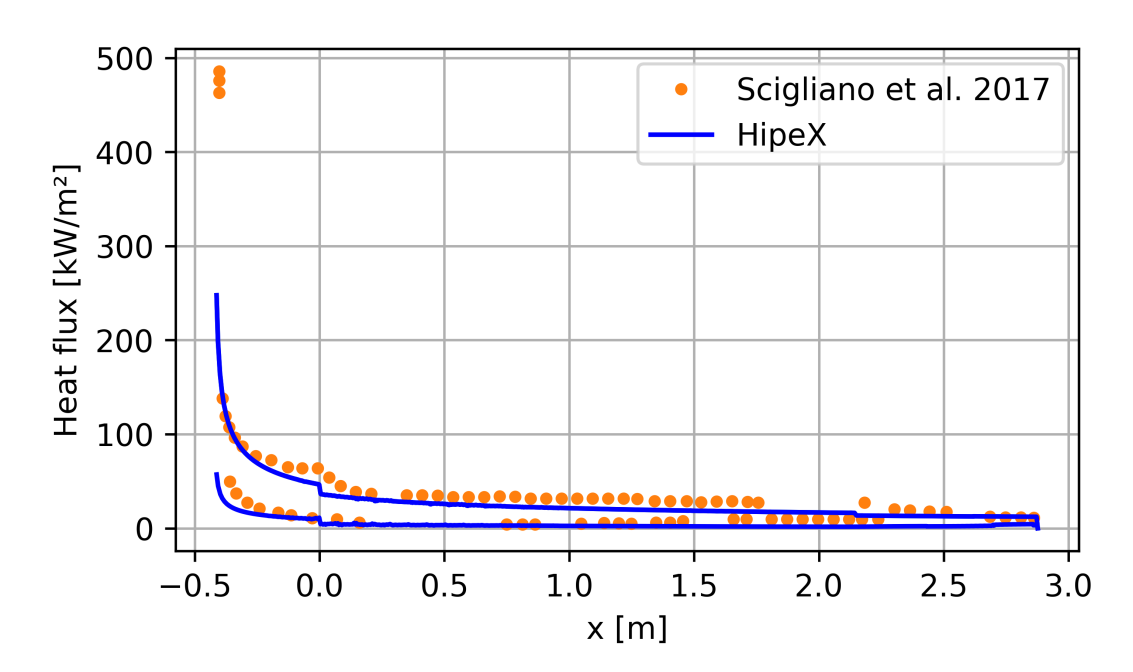


**Fig 7.** Heat flux for M = 7.5, AoA = 12 degrees and 35.9 km of altitude, using the laminar solution.

For the case at Mach 7.25, altitude 29.9 km, and angle of attack of 12 degrees (EFTV-069), heat flux predictions are provided for both laminar and turbulent boundary layer assumptions. Figure 8 presents a comparison of the surface heat flux along the vehicle between HipeX simulations and the ESA reference CFD data. The HipeX laminar prediction closely aligns with the ESA laminar results, while the turbulent model significantly overpredicts the heat flux. The blended solution incorporates a transition model, resulting in a gradual increase in heat flux that bridges the laminar and turbulent extremes. In HipeX, a turbulence intensity of 0.5% is used, which directly influences the transition length. This comparison highlights the advantage of the blended approach in providing more realistic and less overly conservative heat transfer estimates.

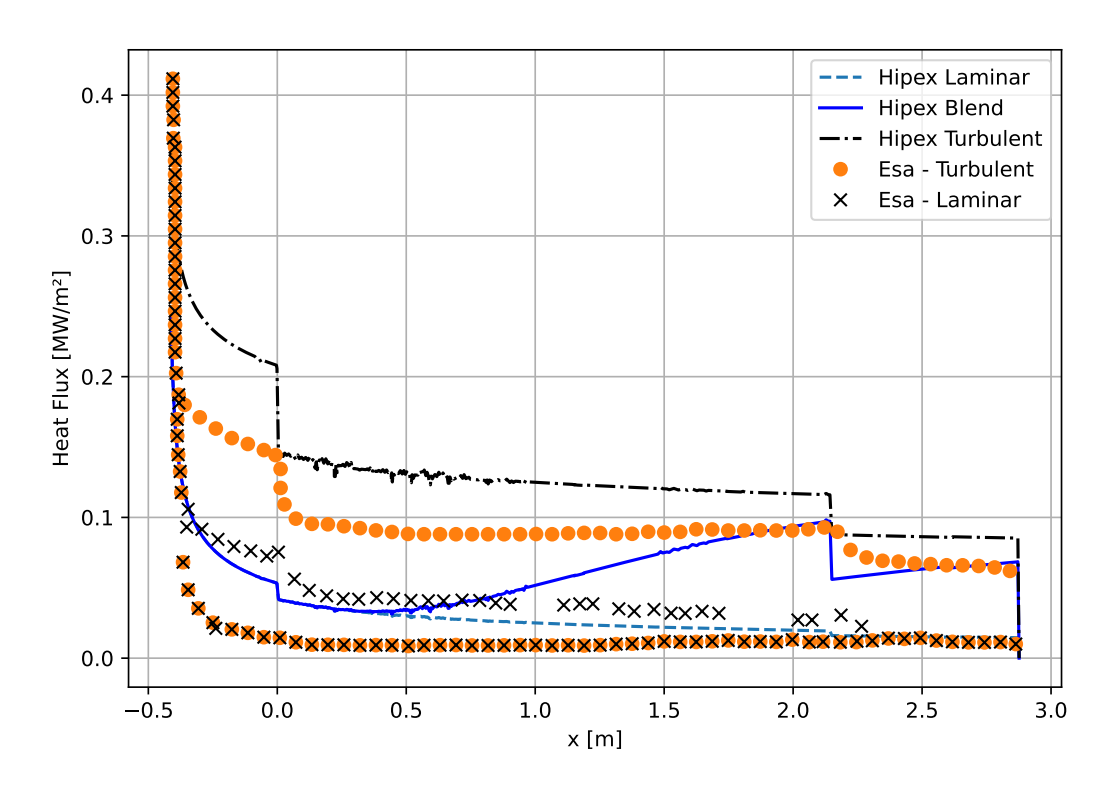


Fig 8. Centerline heat flux for M = 7.25, altitude = 29.9 km and AoA = 12 degrees.

Figure 9 shows the heat transfer prediction for the case at Mach 6.42, altitude 27.4 km, and angle of attack of -1.63 degrees (EFTV-073). The HipeX solution is compared with the fully turbulent reference solution from [17]. In this case, the reference heat flux lies between the HipeX laminar and turbulent predictions, indicating that the actual flow is likely transitional. This further reinforces the value of incorporating a blended boundary-layer model to capture the intermediate behavior typical of high-speed flows undergoing natural transition.

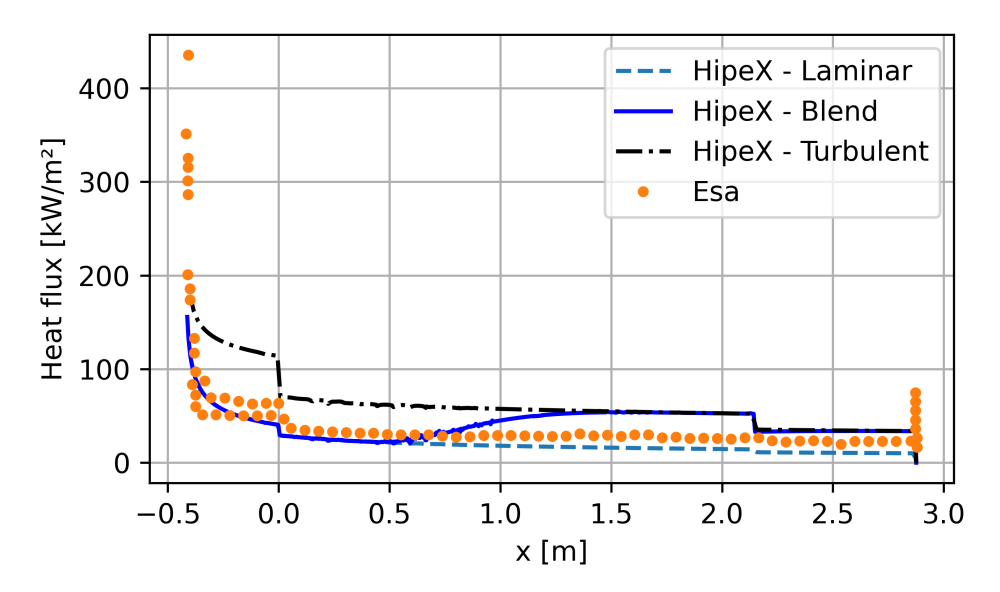
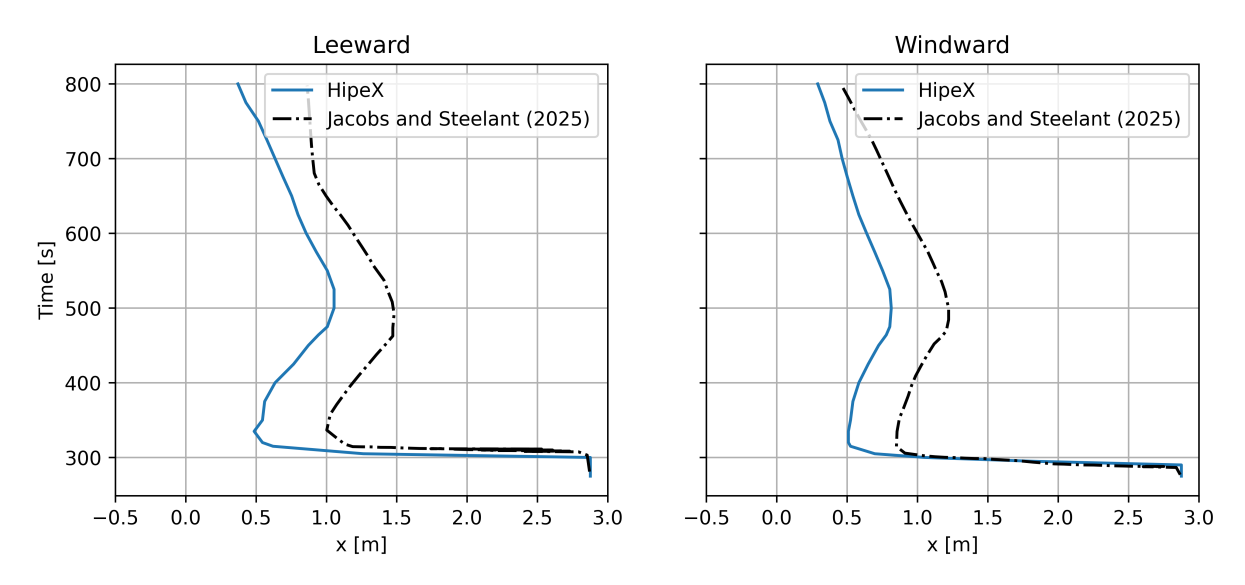


Fig 9. Centerline heat flux for M = 6.42, altitude = 27.4 km and AoA = -1.63 degrees.

## 4. Intermittency comparison

HipeX computes the onset of transition using Equation 19. Figure 10 shows the predicted location of transition onset along the symmetry plane over the reference trajectory from [3]. The results from HipeX and the BLITZ code exhibit similar trends; however, HipeX generally predicts an earlier onset of transition to turbulence compared to BLITZ.



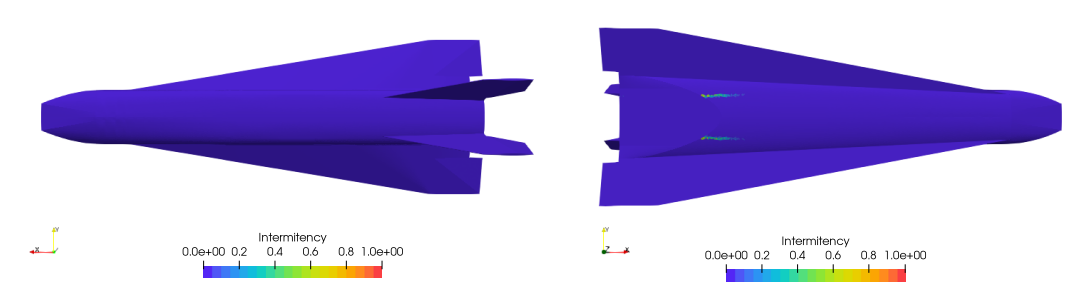
**Fig 10.** Location of the beginning of transition along the flight path.

For 290 s, the flow is majority laminar, in 300 s the HipeX indicates a turbulent region in the windward. For 315 s there is a large turbulent region in the windward and in the leeward. The HipeX needs to be improved to avoid relaminarization. Also, the HipeX do not model the influence of the vertical stabilization in the intermittency on the leeward.

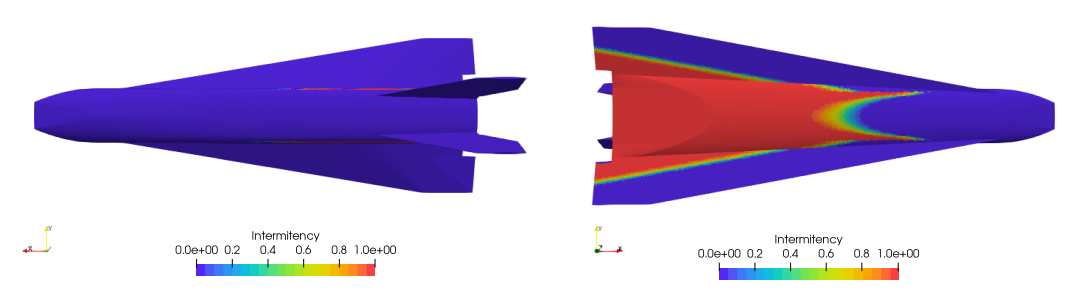
Figure 11 shows the intermittency distribution at different time instants along the trajectory. At t=290 s,

the flow remains predominantly laminar. By  $t=300\,\mathrm{s}$ , HipeX indicates the development of a turbulent region on the windward side. At  $t=315\,\mathrm{s}$ , a significant turbulent region is observed on both the windward and leeward surfaces. A current limitation of the model is the prediction of relaminarization in some expansion regions, which may not be physically accurate.

T = 290 s, M = 7.5, AoA = 12 degrees and 36.25 km of altitude.



T = 300 s M = 7.28, AoA = 12 degrees and 30.13 km of altitude.



T = 315 s, M = 6.94, AoA = 0 degrees and 27.61 km of altitude.

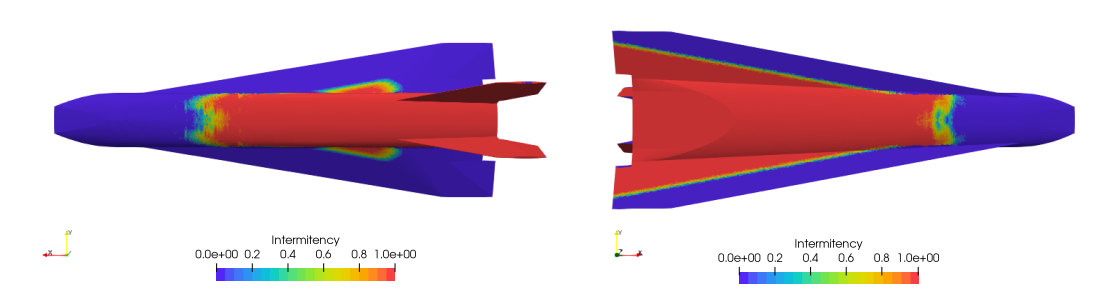


**Fig 11.** Intermittency over the Hexafly surface for different instants of trajectory.

## 5. Conclusion

HipeX demonstrates promising performance in calculating aerodynamic coefficients with good accuracy, especially considering the model's simplicity. It provides reasonable estimations of heat flux for laminar cases, while tending to overpredict heat flux in turbulent scenarios. In most cases, the computational time is under one minute, enabling the rapid evaluation and optimization of numerous geometries during the preliminary design phase.

The implementation of a transition model based on [4] has significantly improved the predictive accuracy

of HipeX, offering less conservative and more realistic results than the fully turbulent assumption. This improvement allows for reduced thermal protection requirements in early design stages, potentially lowering the vehicle's overall weight and fuel consumption.

As discussed, local inclination methods provide fast and robust estimates but are inherently limited. In particular, the approach does not account for boundary layer separation or shock reflections. In some cases, HipeX also predicts relaminarization in expansion regions, which may not be physically accurate. HipeX is a computational tool under active development. Despite its current limitations, it is already a valuable asset for early-stage design studies, offering the capability to assess and optimize a wide range of vehicle configurations with minimal computational cost.

## 6. Acknowledgements

This work was performed within the 'High Speed Experimental Fly Vehicles - International' project fostering International Cooperation on Civil High-Speed Air Transport Research. HEXAFLY-INT, coordinated by ESA-ESTEC, is supported by the EU within the 7th Framework Programme Theme 7 Transport, Contract no.: ACP3-GA-2014-620327. Further info on HEXAFLY-INT can be found on http: //www.esa.int/techresources/hexafly\_int; the 'Technologies for Hypersonic Flights' project, coordinated by the Institute for Advanced Studies, supported by the Brazilian Funding Agency for Studies and Projects (FINEP) under the Contract no.: 01.22.0255.00, by the Brazilian Air Force (COMAER). This work was carried out with the support of the Academic Cooperation Program in National Defense (PROCAD-DEFENSE), grant 88881.387753/2019-01 and by Conselho Nacional de Desenvolvimento Científco e Tecnológico under Grant 307691/2020-9.

#### References

- [1] Pedro Paulo B de Araújo et al. "Local surface inclination method calculations for the HEXAFLY-INT vehicle". In: 3rd International Conference on High-Speed Vehicle Science and Technology (HiSST). 2024.
- [2] Tiago Cavalcanti Rolim, Sheila Cristina Cintra, and Marcela Marques da Cruz Pellegrini. "Development and Application of Computational tool using local surface inclination methods for preliminary analysis of hypersonic vehicles". In: Journal of Aerospace Technology and Management 12 (2020), e2120.
- [3] Frederik Jacobs and Johan Steelant. "Impact of transitional boundary layer evolution on slender high-speed flight vehicles". In: CEAS Space Journal (2025), pp. 1-39. DOI: 10.1007/s12567-025-00639-2. URL: https://doi.org/10.1007/s12567-025-00639-2.
- [4] Maximilian Karsch, Jeroen Van den Eynde, and Johan Steelant. "Linearly combined transition model based on empirical spot growth correlations". In: CEAS Space Journal 15.6 (2023), pp. 947-958. DOI: 10.1007/s12567-023-00499-8. URL: https://doi.org/10.1007/s12567-023-
- [5] United States. National Oceanic, Atmospheric Administration, and United States. Air Force. US Standard Atmosphere, 1976. Vol. 76. 1562. National Oceanic and Atmospheric Administration,
- [6] John David Anderson. Hypersonic and high temperature gas dynamics. Aiaa, 1989.
- [7] John David Anderson. "Modern compressible flow: with historical perspective". In: (No Title) (1990).
- [8] A. Guidi et al. "Implementation of an Aerodynamic Toolbox in a Reentry Flight Simulator". In: Journal of Spacecraft and Rockets 40.1 (2003), pp. 138-141. DOI: 10.2514/2.3929. URL: https://doi.org/10.2514/2.3929.
- [9] ERG Eckert. Engineering relations for friction and heat transfer to surfaces in high velocity flow. 1955. DOI: 10.1115/1.4014011. URL: https://doi.org/10.1115/1.4014011.
- [10] Kevin G Bowcutt, John D Anderson, and Diego Capriotti. "Viscous optimized hypersonic waveriders". In: 25th AIAA Aerospace Sciences Meeting. 1987, p. 272. DOI: 10.2514/6.1987-272. URL: https://doi.org/10.2514/6.1987-272.

- [11] Sara Di Benedetto et al. "The high-speed experimental flight test vehicle of HEXAFLY-INT: a multidisciplinary design". In: *CEAS Space Journal* 13 (2021), pp. 291–316. DOI: 10.1007/s12567-020-00341-5. URL: https://doi.org/10.1007/s12567-020-00341-5.
- [12] Johan Steelant et al. "Flight testing designs in HEXAFLY-INT for high-speed transportation". In: Proceedings of HiSST (2018).
- [13] Sil van Brummen et al. "Aerodynamic design analysis of the HEXAFLY-INT hypersonic glider". In: 20th AIAA International Space Planes and Hypersonic Systems and Technologies Conference. 2015, p. 3644.
- [14] Antonio Schettino et al. "Aerodynamic database of the HEXAFLY-INT hypersonic glider". In: *CEAS Space Journal* 12 (2020), pp. 295–311. DOI: 10.1007/s12567-020-00299-4. URL: https://doi.org/10.1007/s12567-020-00299-4.
- [15] Roberto Scigliano et al. "HEXAFLY-INT experimental flight test vehicle (EFTV) aero-thermal design". In: ASME International Mechanical Engineering Congress and Exposition. Vol. 58349. American Society of Mechanical Engineers. 2017, V001T03A022. DOI: 10.1115/imece2017-70392. URL: https://doi.org/10.1115/imece2017-70392.
- [16] Johan Steelant et al. "Numerical and experimental research on aerodynamics of a high-speed passenger vehicle within the HEXAFLY-INT project". In: *ICAS 2016 Proceedings* (2016).
- [17] Roberto Scigliano et al. "Aerothermal Design of the Hexafly-int Glider". In: AIAA SPACE 2016. Aiaa, 2016. DOI: 10.2514/6.2016-5627. URL: https://arc.aiaa.org/doi/abs/10.2514/6.2016-5627.